VILNIAUS UNIVERSITETAS

MATEMATIKOS IR INFORMATIKOS FAKULTETAS

Master thesis

Functional data analysis of regional brain neurophysiological activity influenced by chronic ethanol consumption

Smegenų centrų, paveiktų chroniško etanolio vartojimo, neurofiziologinės veiklos tyrimas taikant funkcinės duomenų analizės metodus

Tadas Danielius

VILNIUS 2018

Darbo vadovas prof. habil. dr. Alfredas Račkauskas

Darbo recenzentas dr. Jurgita Markevičiūtė

Darbas apgintas 2018 sausio 15

Darbas įvertintas _____

Registravimo Nr. 111000-9.1-5/_____

2018-01-05 _____

Functional data analysis of regional brain neurophysiological activity influenced by chronic ethanol consumption

Abstract

Lamotrigine with anti-glutamatergic properties may have potential utility as novel treatments for alcoholism. Nevertheless, to which extent different neurotransmitter systems contribute to the development of behavioural inflexibility in alcoholism is not entirely clear. In order to understand it better understand it, behavioural animal model of long-term voluntary alcohol taking behaviour experiment was done. In this study functional data analysis of recorded neurophysiological data revealed that the third functional principal component (PC) had significant changes during drinking bout, while animal was injected with lamotrigine. Analysis of PCs showed that background brain process accounted for roughly 60% of variability. After applying VARIMAX rotation, PCs highlighted time segments, which may help to understand brain dynamics leading to decision making process in brains. Continuous wavelet transform analysis of the third PC display 4 times stronger power spectrum levels when animal was injected with drug.

Key words : Functional Data Analysis, Functional Principal Component Analysis, VARIMAX, Continuous Wavelet transform, Nucleus Accumbens, rat brains, lamotrigine

Smegenų centrų, paveiktų chroniško etanolio vartojimo, neurofiziologinės veiklos tyrimas taikant funkcinės duomenų analizės metodus

Santrauka

Lamotriginas priklauso vaistų su anti-glutamatogerinėmis sąvybėmis grupei, todėl manoma, kad šis preparatas galbūt galėtų būti taikomas ir alkoholizmui gydyti. Visgi nėra aišku, kurių neuromediatorių įtaka elgesio kontrolės praradimui yra didžiausia. Todėl buvo atliktas tyrimas siekiant geriau suprasti alkoholio vartojimo sąlygotą poveikį specifinėms galvos smegenų sritims ir ištirti elgesio kontrolės praradimo priežastis. Šiame darbe surinkti neurofiziologiniai duomenys buvo analizuojami funkcinės duomenų analizės metodais. Analizės rezultatai parodė, kad trečioji funkcinė principinė komponentė turi stipriausius pokyčius gėrimo metu tuo atveju, kai gyvūnui buvo suleisti vaistai. Taip pat analizuojant principines komponentes buvo nustatyta, kad bendras smegenų foninis darbas sudaro apie 60% dispersijos. Atlikus principinių komponenčių VARIMAX rotaciją buvo nustatyti laiko segmentai, galintys padėti suprasti smegenų procesus, atsakingus už sprendimą gerti alkoholį ar ne. Tolydžios vilnelės transformacijos analizės principais buvo nustatyta, kad trečioji komponentė turi 4 kartus stipresnį energijos dažnių spektrą tuo atveju, kai gyvūnams buvo suleisti vaistai.

Raktiniai žodžiai : Funkcinė duomenų analizė, funkcinės principinės komponentės, VARIMAX, tolydi vilnelės transformacija, Nucleus Accumbens, žiurkių smegenys, lamotriginas

Contents

List of Figures

Abbreviations

CNS Central Nervous System. 8

CPu Caudate Putamen. 13, 24

CWT Continuous Wavelet Transform. 3, 5, 6, 12, 13, 16, 21, 22, 32

DWT Discrete Wavelet Transform. 8

EEG Electroencephalography. 3, 6, 8, 12

EPSP Excitatory Postsynaptic Potential. 7

FDA Functional Data Analysis. 5, 6, 8, 9, 11, 16, 19

FFT Fast Fourier transform. 6, 8

fPCA Functional Principal Component Analysis. 5, 6, 10, 11, 17, 18, 24

FT Fourier transform. 8, 11

GABA Gamma Amino Butyric Acid. 7

IPSP Inhibitory Postsynaptic Potential. 7

LFP Local Field Potentials. 12, 15

Nac Nucleus Accumbens. 5, 13

NMDA N-methyl-D-aspartate. 7, 8

PC Principal Component. 3, 11, 16–24, 29–33

PCA Principal Component Analysis. 5, 17

PEG Polyethylene Glycol. 3, 14, 21, 22, 24, 28, 30

PSP Post-synaptic potentials. 7

1 Introduction

There is a growing evidence that medications such as lamotrigine with anti-glutamatergic properties currently in clinical use may have potential utility as novel treatments for alcoholism. Nevertheless, to which extent different neurotransmitter systems contribute to the development of behavioural inflexibility in alcoholism is not entirely clear. For this reason, behavioural animal model of long-term voluntary alcohol taking behaviour experiment was done and neurophysiological data was recorded. Which sets the primary goal of this study: find out if voluntary chronic alcohol consumption can be monitored as neurphysiological activity changes in Nucleus Accumbens (Nac) brain area with and without lamotrigine injected. Brain is obviously a complex system and exhibits rich spatiotemporal dynamics. Complex neuronal electrical activity generates irregular neurophysiological signals that translate into seemingly random and ever-changing brain waves. Since there is no definite criterion evaluated by the experts, visual analysis of recorded brain signals is insufficient, making it a interdisciplinary challenge to find physiological explanation of characteristics and patterns observed in electrical signals.
Fortunately, the nature of the underlying process generating the data is smooth and adjacent points measured along the continuum are not independent, therefore can be treated as functional observations making Functional Data Analysis (FDA) a splendid technique for this analysis. In this study expressions such as Principal Component Analysis (PCA) and correlations are used in the functional domain. Functional Principal Component Analysis (fPCA) is used to extract components, which are responsible for different processes encoded in the electrical brain signals. The process separation helps estimate the variability of background processes along with noise, whilst allowing to analyze specific processes independently. Applying Continuous Wavelet Transform (CWT) on independent principal components reveals the presence of potential frequency changes across the time. Finally, concepts of cross-wavelet analysis provide versatile statistical methods for frequency content comparison across certain ranges of time.

1.1 Objective of the Thesis

The purpose of this thesis is twofold. On a statistical level using FDA and CWT as techniques for exploring neurophysiological data and drawing the conclusions. On a conceptual level is to evaluate the effect of the drug by digging into brain activity recorded from rat brains during experiment. Considering these aims in more detail the purpose is to understand how neurophysiological data can be analyzed using FDA and CWT to detect the influence of active substance in the brain activity, by separating different processes. Secondly, is to step into neuroscience and provide a glimpse of the brain signals and how such signals are interpreted, which is well known to neuroscientists, but, generally, unknown to statisticians.

1.2 Thesis outline

The thesis is organized as follows:

- *Introduction* is made of a short presentation of the context the problem definition and an overview of the structure of the thesis.
- *Background* covers essentials about the origin of electrical brain signals, neurotransmitters and how they are affected by drug. It also, explains brain wave frequencies and why they are important when interpreting findings.

- *Literature Review* covers an overview of recent studies and findings from both neuropharmacological and statistical perspective.
- *Functional Data analysis* covers theoretical concepts and mathematical background of FDA.
- *Continuous wavelet transform* constitutes a sequel of mathematical background of the previous chapter by introducing theory of CWT, explaining the concepts time-frequency analysis as well as scaling and shifting mechanisms.
- *Materials and methods* explains the experiment, data, analysis and visualization. In analysis sections emphasize techniques such as fPCA, VARIMAX rotation of fPCA, coherence of frequency contents, followed by discussion.
- *Conclusions* presents the conclusions drawn and future perspectives.

2 Background

In order to understand the experiment and conclusions some background information is needed. This chapter gives a brief introduction to the brain electrical activity, glutamate system and frequencies.

2.1 Brain waves frequency

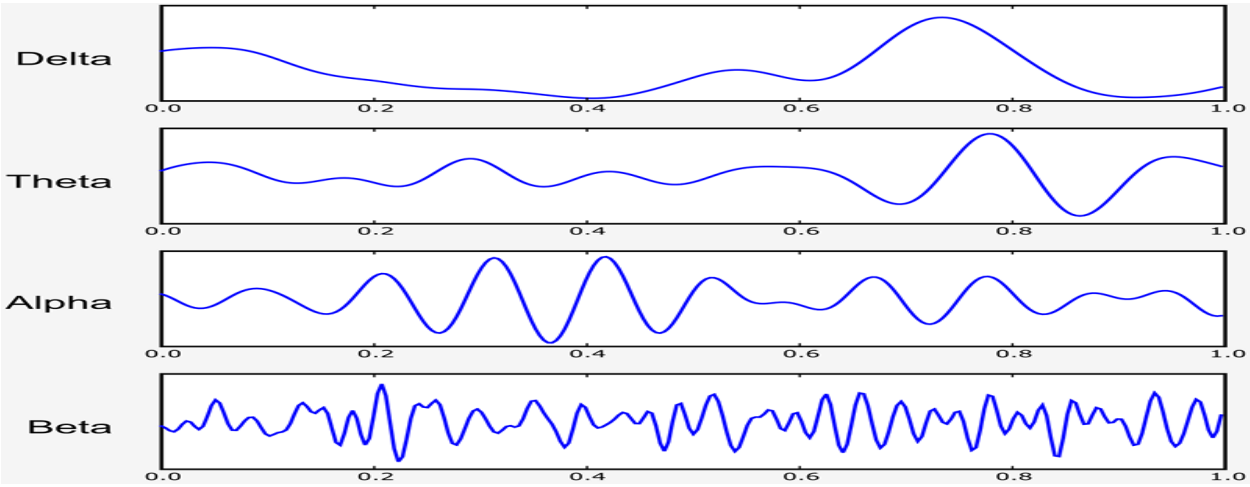

Figure 1: Electroencephalography (EEG) frequency bands. Source [1].

Frequency refers to the rate at which a waveform repeats its cycle within 1 second. Frequency analysis, that is, analyzing the neurophysiological signal in terms of the range of its frequencies, was traditionally of two basic types: spectral analysis by narrowband filters by dividing the signal into 1Hz segments or bins or by wideband electronic filters [2] [3]. Spectral analysis is concerned with the exploration of cyclical patterns of data. The purpose of the analysis is to decompose a complex time series with cyclical components into a few underlying sinusoidal functions of particular wavelengths. Most common method of analyzing the frequency of the spectrum is to use the Fast Fourier transform (FFT). The results of spectral analysis of a complex waveform such as EEG or neurophysiological recordings are measures of the amount of energy distributed in a frequency bands of the waveform. The EEG is traditionally categorized into a handful of different frequency bands

1. Delta (δ): 1–3.5 Hz;
2. Theta (θ): 4–7.5 Hz;
3. Alpha (α): 8–12 Hz;
4. Sigma (σ): 13-16 Hz;
5. Beta (β): 16.5–25 Hz;
6. Gamma (γ): 30–35 Hz.

Activity that falls into the δ or θ bands is referred to as *slow-wave activity* and activity falling into the α or β bands is referred to as *fast-wave activity*. Figure 1 shows four frequency bands (α, β, θ and δ) which are explored in most cases.
In neuroscience community it is common practice to explain physiological rhythmic characteristics by comparing energy of frequency bands. Whatever it may be caused by stimulus response or other elements which may contribute to energy distribution changes. As such, it places restrictions on how signal can be manipulated, yet to retain that information for final interpretation.

2.2 Brain electrical activity

There are two broad classes of cells in the nervous system: *neurons*, which process information, and *glia*, which provide the neurons with mechanical and metabolic support. The neuron's basic parts are cell body (soma), axion, and dendrites. The cell body contains the organelles of the cell including the nucleus, golgi apparatus (metabolic center) and endoplasmic reticulum. Most of what is recorded originates from neurons and there is a number of possible sources including action potentials, post-synaptic potentials and chronic neuronal depolarization. Action potentials induce a brief 10ms or shorter local current in the axon with a very limited potential field. Post-synaptic potentials (PSP) are considerably longer (50-200ms) and have a much greater field. Normally brain action potentials travel down to axon to the nerve terminal where a neurotransmitter is released. At the post-synaptic membrane the neurotransmitter produces a change in membrane conductance and transmembrane potential. The chemicals emitted from the synaptic junctions can either excite (depolarize) or inhibit (hyper-polarize) the neural membrane. If the signal has an excitatory effect on the neuron it results in influ of positive charge and establishes an Excitatory Postsynaptic Potential (EPSP). They are small, typically located in the dendrites, usually 5 mV and are not sufficient to trigger an action potential. However, most neurons are multipolar, and thus have many dendrites whose inputs create a summation sufficient of EPSP enough to trigger an action potential. An Inhibitory post-synaptic potentials result in local hyperpolarization (about 20 inhibitory neurotransmitters such as Gamma Amino Butyric Acid (GABA)) leading to intracellular negativity. In this way the cell becomes inhibited from firing; that is, an Inhibitory Postsynaptic Potential (IPSP) is created. The combination of EPSPs and IPSPs induces **currents** that flow within and around the neuron with a potential field sufficient to be recorded.

2.3 Glutamate receptors and Lamotrigine mechanism of action

The **N-methyl-D-aspartate (NMDA)** receptor is a glutamate receptor and ion channel protein found in nerve cells. Glutamate is the major brain's excitatory neurotransmitter and also the precursor for GABA, the brain's main inhibitory neurotransmitter in the nervous

system [4]. It is a chemical that nerve cells use to send signals to other cells.
Lamotrigine is a member of the sodium channel blocking class of antiepileptic drugs [5]. This may suppress the release of glutamate and aspartate, two of the dominant excitatory neurotransmitters in the Central Nervous System (CNS) [6]. Studies suggest that lamotrigine acts presynaptically on voltage-gated sodium channels to decrease glutamate release.
Glutamate system is important in the neural and behavioral actions of alcohol and the processes driving the development of alcoholism.

3 Literature Review

Two different topics were investigated: from neuropharmacological perspective to understand the effect of anti-glutamatergic properties and from computational neuroscience perspective to investigate existing statistical methods currently used for EEG analysis
There is a growing evidence that the glutamate system is important in the neural and behavioral actions of alcohol and the processes driving the development of alcoholism [7]. Compounds with anti-glutamatergic properties in clinical use for various indications (e.g. Alzheimer's disease, epilepsy, psychosis, mood disorders) have potential utility as novel treatments for alcoholism. Enhanced sensitivity to certain acute intoxicating effects (ataxia, sedative) of alcohol may be one mechanism by which anti-glutamatergic drugs modulate alcohol use [7]. Recent research indicates the involvement of the glutamatergic system in mediating acute and chronic alcohol effects [8]. Neurons exposed chronically to ethanol are significantly more susceptible to glutamate-induced neuronal death mediated by the NMDA receptor. Several studies demonstrated that ethanol-dependent experimental animals were much more sensitive to the neurotoxic consequences of treatment with NMDA receptor agonists [9] [10] [11].
Different approaches were studied to support such claims, but the effect on electrical brain activity in different brain regions to current knowledge is not known.
Many methods were proposed for EEG analysis. Most common method is computation of the FFT for spectral analysis [12]. FFT transforms a signal from the time domain into the frequency domain. The relatively simple method can reveal hidden features of noisy EEG recordings and a conveniently plotted in a frequency power-spectrum. However, it is very sensitive to large noise [13] and is not localized in time. Also, Fourier transform (FT) does not represent abrupt changes efficiently. The reason for that is that the FT represents data as a sum of sine waves which are not localized in time. These sine waves oscillate infinitely. Other proposed technique assume that potentials can be analyzed using linear statistics [14]. however, approximation of signals should rely on nonlinear methods [15]
In more recent studies Discrete Wavelet Transform (DWT) is becoming more popular since it captures both frequency and location information (e.g. [16] [17] [18] [19]).
Examination of literature shows that many practical and accurate methods already exists. However, these techniques are seldom applied in clinical examination, particularly on electrical signals from brain activity.

4 Functional Data analysis

FDA is a well-established major branch of statistics and is becoming widely adopted across many disciplines. The roots of its development can be tracked back to around 1800 when Gauss and Legendre were trying to estimate a comet's trajectory. It is rapidly evolving in methodology as well as applications since it was made well known by Ramsay & Silverman's monograph in 1997. Instead of discrete points as commonly analyzed in classical statistics,

the general form of each sample element is considered to be a function. The physical continuum over which these functions are defined is often time. Since scientists today often collect samples of curves and other functional observations, FDA makes a versatile tool for analysis. Also, most of the methods used in classical statistics have their counterparts in the concept of FDA. Generally, functional data are a natural generalization of multivariate data from finite dimensional to infinite dimensional.
Let, the functional datum arrives as a finite set of measured values, $y_1, \ldots, y_n$. Further, assume that there is a reasonably smooth function $x_i(t)$ that gives rise to those measured values, then the model can be defined as

$$y_j = x(t_j) + \epsilon_j \tag{1}$$

with t in a continuum (usually time), y_j is the jth observation and ϵ_j is error or residual. Function $x(t)$ is constructed using a system of basis functions, which is a linear combination of K independent of each other basis expansion functions denoted by $\phi_k(t)$ for $k = 1, \ldots, K$. That is

$$x(t) = \sum_{k=1}^{K} \alpha_k \phi_k(t) = \mathbf{A}^\top \mathbf{\Phi}(t)$$

where $\mathbf{A} = [\alpha_1, \ldots, \alpha_K]$ is a coefficients vector of length K and $\mathbf{\Phi}(t)$ is the K-vector basis functions. The vector format of formula (1) can be written as

$$\mathbf{y} = x(\mathbf{t}) + \epsilon$$

where $\mathbf{y}$, $\mathbf{t}$ and ϵ are all column vectors of length n.
When constructing such functions it is important to define the number of basis functions K. The larger K, the better fit to the data, however there is a risk fitting noise or variation which is not needed. On the other hand, choosing K too small may loose important aspects of the smooth function x which is required to estimate.
The other element to consider is a choice of basis functions to use. Basis functions are a set of mathematically independent functions, denoted by $\phi_k(t)$, that are combined and used to estimate any function $x(t)$. Understanding the underlying behaviour of the data may help to choose the basis functions which serves better for modelling the process. Mainly two basis functions are used: *Fourier* series which are better for periodic data and most popular *b-spline* basis system [20].
For the b-spline smoothing theoretical background is provided, since it is applied in this study. The chapter 6 discusses the motivation behind the reason why b-spline is more appropriate choice than Fourier basis.

4.1 B-spline Smoothing

The term "B-spline" was coined by *Isaac Jacob Schoenberg* and is short for basis spline [20] A spline function of order m is a piecewise polynomial function of degree $m-1$ in a variable x. The places where the pieces meet are known as *knots*.
A B-spline is a generalization of the *Bézier curve*. Let a vector known as the knot vector be defined

$$T = \{t_0, t_1, \ldots, t_m\},$$

where T is non decreasing sequence with $t_i \in [0, 1]$, and define control points $P_0, \ldots, P_n$. Define the degree as

$$p \equiv m - n - 1.$$

The "knots" $t_{p+1}, \ldots, t_{m-p-1}$ are called internal knots. Define the basis functions as

$$B_{i,0}(x) := \begin{cases} 1 & \text{if} \quad t_i \leq x < t_{i+1} \\ 0 & \text{otherwise} \end{cases}$$

$$B_{i,k}(x) := \frac{x - t_i}{t_{i+k} - t_i} B_{i,k-1}(x) + \frac{t_{i+k+1} - x}{t_{i+k+1} - t_{i+1}} B_{i+1,k-1}(x).$$

where $k = 1, 2, \ldots, p$. Then the curve defined by

$$\phi(t) = \sum_{i=0}^{n} P_i B_{i,p}(t)$$

is a B-Spline.
The linear smoother is obtained by adjusting the coefficients of the expansion α_k in order to minimize the least squares criterion between raw data and weighted bases ϕ_k [21]

$$SMSSE(y|\alpha) = \sum_{j=1}^{n} [y_j - \sum_{k=1}^{K} \alpha_k \phi_k(t_j)]^2$$

This can be rewritten in a matrix form as

$$SMSSE(\mathbf{y}|\mathbf{A}) = (\mathbf{y} - \mathbf{\Phi A})^\top (\mathbf{y} - \mathbf{\Phi A}).$$

where A is the coefficient vector of length K, $\mathbf{\Phi}$ is the $n \times K$ matrix including the values $\phi_k(t_j)$, and $\mathbf{y}$ is the n-vector of discrete data points.
Taking the derivative of criterion $SMSSE(\mathbf{y}|\mathbf{A})$ with respect to $\mathbf{A}$ yields the equation [21]

$$2\mathbf{\Phi}\mathbf{\Phi}^\top \mathbf{A} - 2\mathbf{\Phi}^\top \mathbf{y} = 0$$
$$\hat{\mathbf{A}} = (\mathbf{\Phi}\mathbf{\Phi}^\top)^{-1} \mathbf{\Phi}^\top \mathbf{y}.$$

Solving equation for $\mathbf{A}$ provides estimate $\hat{\mathbf{A}}$ that minimizes the least square solution.

4.2 Functional principal component analysis

A key technique to consider when analysing functional data is *Functional Principal Component Analysis*. Using this method, a random function is represented in the eigenbasis, which is an orthonormal basis of the Hilbert space L^2 that consists of the eigenfunctions of the autocovariance operator. It represents functional data in the most parsimonious way, in the sense that when using a fixed number of basis functions, the eigenfunction basis explains more variation than any other basis expansion.
For a square-integrable stohastic process $X(t), t \in T$, let

$$\mu(t) = \mathrm{E}(X(t))$$

and

$$G(s,t) = \mathrm{Cov}(X(s), X(t)) = \sum_{k=1}^{\infty} \lambda_k \varphi_k(s) \varphi_k(t)$$

where $\lambda_1 \geq \lambda_2 \geq \cdots \geq 0$ are eigenvalues and $\varphi_1(t), \varphi_2(t), \ldots$ are the orthonormal eigenfunctions of the linear Hilbert–Schmidt operator

$$G : L^2(\mathcal{T}) \to L^2(\mathcal{T}),\ G(f) = \int_{\mathcal{T}} G(s,t)f(s)ds.$$

By the Karhunen–Loève theorem, one can express the centered process in the eigenbasis,

$$X(t) - \mu(t) = \sum_{k=1}^{\infty} \xi_k \varphi_k(t),$$

where

$$\xi_k = \int_{\mathcal{T}} (X(t) - \mu(t))\varphi_k(t)\, dt \tag{2}$$

is the Principal Component (PC) associated with the k-th eigenfunction φ_k, with the properties $\mathrm{E}(\xi_k) = 0, \mathrm{Var}(\xi_k) = \lambda_k$ and $\mathrm{E}(\xi_k\xi_l) = 0$ for $k \neq l$.

The centered process is then equivalent to $\xi_1, \xi_2, \ldots$. A common assumption is that X can be represented by only the first few eigenfunctions (after subtracting the mean function), i.e.

$$X(t) \approx X_m(t) = \mu(t) + \sum_{k=1}^{m} \xi_k \varphi_k(t),$$

where

$$\mathrm{E}\left(\int_{\mathcal{T}} (X(t) - X_m(t))^2\, dt\right) = \sum_{j>m} \lambda_j \to 0 \text{ as } m \to \infty.$$

The first eigenfunction φ_1 depicts the dominant mode of variation of X.

$$\varphi_1 = \underset{\|\varphi\|=1}{\arg\max} \left\{ \mathrm{Var}(\int_{\mathcal{T}} (X(t) - \mu(t))\varphi(t)dt) \right\},$$

where

$$\|\varphi\| = \left(\int_{\mathcal{T}} \varphi(t)^2 dt\right)^{\frac{1}{2}}.$$

The k-th eigenfunction φ_k is the dominant mode of variation orthogonal to $\varphi_1, \varphi_2, \ldots, \varphi_{k-1}$,

$$\varphi_k = \underset{\|\varphi\|=1, \langle\varphi,\varphi_j\rangle=0 \text{ for } j=1,\ldots,k-1}{\arg\max} \left\{ \mathrm{Var}(\int_{\mathcal{T}} (X(t) - \mu(t))\varphi(t)dt) \right\},$$

where

$$\langle \varphi, \varphi_j \rangle = \int_{\mathcal{T}} \varphi(t)\varphi_j(t)dt, \text{ for } j = 1, \ldots, k-1.$$

In statistical literature fPCA received considerable attention. It plays much more central role in FDA than similar techniques in multivariate analysis.

5 Continuous wavelet transform

Fourier analysis is a popular method which allows to study the cyclic nature of a time series in the frequency domain. However, under FT the time information of time series is discarded. Thus, making impossible to distinguish transient relations or to identify when structural changes do occur. In addition to that, these techniques are only appropriate for the analysis of time series, which has stable statistical properties and is stationary. It is well-known that

neural data, including EEG and Local Field Potentials (LFP), can be highly non-stationary, exhibiting large fluctuations in both mean and variance over time.
To overcome this limitation wavelet analysis was proposed. It performs the estimation of the spectral characteristics of a time series as a function of time. These techniques make it possible to reveal how different periodic components of the time series change over time.
Wavelet theory is one of the most modern areas of mathematics. Originally developed by French researchers, such as Yves Meyer, Stéphane Mallat and Albert Cohen. As analytical tool it is now widely used in many areas of technical research Seasoned achievements in computer science, medicine, biology were made. George Zweig, a former particle physicist who turned to neurobiology, introduced the CWT [22]. CWT maps time series, which is function of time into function of two variables: time and frequency. Electrophysiological processes generally exhibit oscillatory structure making them well suited for frequency-domain analysis [23].

5.1 Wavelets

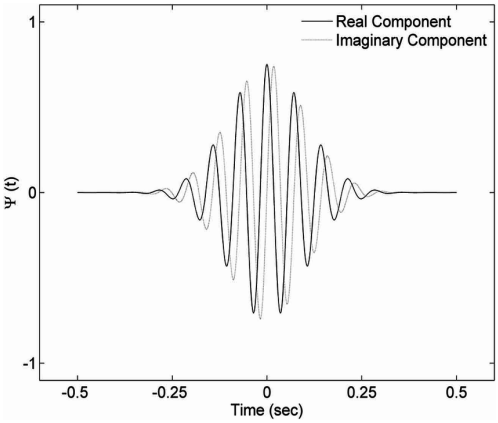

(a) Complex Morlet wavelet with central frequency $f_0 = 2$.

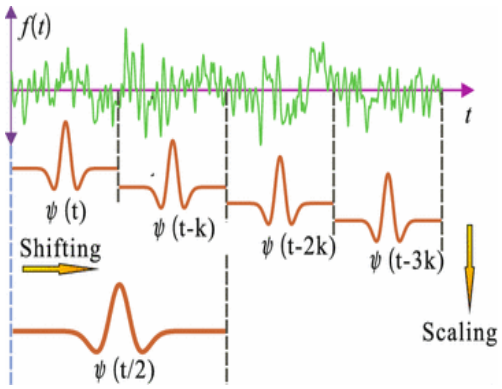

(b) Wavelet scaling and shifting (source [24])

Wavelet is a rapidly decaying wave like oscillation that has zero mean Technically, wavelet is a function with an amplitude which begins at zero, increases over time and decreases to zero. Function $\psi(t) \in L^2(R)$ is defined as a *mother wavelet* if it satisifies following condition usually referred as *admissibility condition*:

$$0 < C_\psi := \int_{-\infty}^{\infty} \frac{|\Psi(w)|}{|w|}\, dw < \infty. \tag{3}$$

Admissibility condition (3) is equivalent to requiring that

$$\Psi(0) = \int_{-\infty}^{\infty} \psi(t)\, dt = 0.$$

The wavelet used in this study is known as Morlet (figure 2a). While studying reflection seismology Morlet observed that, instead of emitting pulses of equal duration, shorter waveforms at high frequencies should perform better in separating the returns of fine closely-spaced layers [22].

5.2 Definition

The CWT of a signal $x(t)$ at a scale (s>0) $s \in \overline{\mathbb{R}}^+$ and translational value $\tau \in \mathbb{R}$ is defined by [25]

$$\Phi(\tau, s) = \frac{1}{|s|^{1/2}} \int_{-\infty}^{\infty} x(t) \overline{\psi} \left(\frac{t-\tau}{s} \right) dt \tag{4}$$

where

$$\psi(t) = \pi^{-1/4} e^{iwt} e^{-t^2/2} \tag{5}$$

is a continuous function (see figure 2a) in both the time domain and the frequency domain called the mother wavelet; the over-line ($\overline{\psi}$) represents operation of *complex conjugate*.
There are two import wavelet transform concepts: scaling and shifting Scaling refers to the process of stretching or shrinking the signal in time which can be expressed using $\psi(t/s), s > 0$. The scale factor is inversely proportional to frequency. Stretched wavelet helps capturing the slowly varying changes in a signal while a compressed wavelet helps capturing the abrupt changes. Shifting a wavelet simply means delaying or advancing the onset of the wavelet along with the length of the signal. A shifted wavelet represented by $\psi(t-\tau)$ means that the wavelet is shifted and centered at τ. Shifting the wavelet aligns with the feature of interest for the signal. Figure 2b demonstrates the scaling and shifting. The choice of the set of scales s determines the wavelet coverage of the series in the frequency domain. The scale value is fractional power of 2.

6 Materials and methods

The goal of the experiment is to get a better insight on the anatomical and functional basis of the loss of control over alcohol taking behaviour and continuation of alcohol consumption. To fulfil this goal the behavioural animal model of long-term voluntary alcohol taking behaviour was used. Data were collected during experiment carried out with ten two-month-old male Wistar rats (from breeding colony at the Vilnius University, Vilnius, Lithuania). All animals were housed individually in standard rat cages under a 12/12-hour artificial light/dark cycle (lights on at 7:00 a.m.). Experiments targeted four different brain areas.

1. Nucleus Accumbens (Nac)
2. Caudate Putamen (CPu)
3. Orbitofrontal cortex (OFC)
4. Anterior cingulate cortex (ACC)

Rats were divided into two separate groups. Rats belonging to the first group were given free choice to drink either water with 10% ethanol or tap water during whole experiment. Animals had opportunity to drink alcohol for at least two months before neurophysiological measurements took place. After this period only rats who consumed no less than 2g pure alcohol per 1 kg body weight per one day were selected for further studies. The second (control) group of rats were never exposed to the alcohol and only had access to the tap water. After two month period control and chronically drinking rats had surgery and recording electrodes were attached to the different regions of the brain. This study focuses only on Nac brain center. Each rat participated in at least three trials:

- Trial 1: Rat was not given any drugs or substances. Only sodium chloride concentration of 10% were injected.

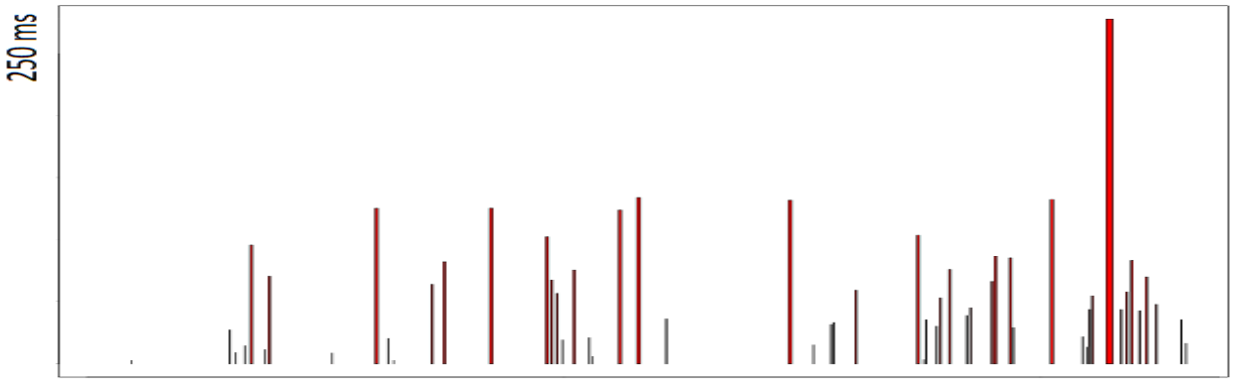

Figure 3: Lickometer data for rat 1 during 24h. x axis represents time and y axis represents "lick" duration in ms.

- Trial 2: Rat was injected with Polyethylene Glycol (PEG) for control test.
- Trial 3: Lamotrigine was dissolved in PEG and then diluted with water to a final PEG concentration of 20%. The solution was freshly prepared and injected as a volume of 5ml/kg intraperitoneally (IP).

6.1 Data

During the experiment two processes were recorded:

1. The optical Lickometers were used to measure licking/drinking from a standard drinking tube
2. Neurophysiological signals

6.1.1 Lickometer data preparation

Lickometer apparatus were used in these experiments to record fluid intake continuously during trial. The format of lickometer data was saved in a tuple form $Y^{(n)} = (t, a)$ form, where n is lickometer number, t is timestamp when lickometer was triggered and a is event indicating ON or OFF action. Normally the first event indicates ON event following by OFF event after short period of time. Data had to be prepared in a suitable form for further analysis. Dataset had to be split into two vectors:
$v^{(n)} = [Y^{(n)}_{(1,1)}, Y^{(n)}_{(3,1)}, \cdots, Y^{(n)}_{(k-1,1)}]^\top$ and $\ddot{v}^{(n)} = [Y^{(n)}_{(2,1)}, Y^{(n)}_{(4,1)}, \cdots, Y^{(n)}_{(k,1)}]^\top$ where $v^{(n)}$ contains ON actions and $\ddot{v}^{(n)}$ contains OFF actions. Duration can be calculated as

$$\Delta^{(n)} = \ddot{v}^{(n)} - v^{(n)}$$

To better understand the information captured figure 3 displays lickometer activity for the rat 1. It is clear that, when rat was drinking from the tube, many times event was triggered with each lick, thus separate licks had to be combined to form clusters, which were treated as a drinking bout. A bout is defined as at least 20 licks, with no more than a minute between licks [26]. The bout definition was also used for ethanol drinking bout analysis in previous studies [27]. The aggregation procedure can be defined as

$$f^{(n)}(t) = \begin{cases} 1 & \text{if} \quad t \in [v_i^{(n)}, \ddot{v}_i^{(n)}] \quad \text{for} \quad 0 < i < N \\ 0 & \text{otherwise} \end{cases}$$

where N is a number of total records in dataset for lickometer n.
Let,

$$\underline{F}^{(n)}(t) = \sum_{i=t}^{t+30} f^{(n)}(i),$$

$$\overline{F}^{(n)}(t) = \sum_{i=t}^{t-30} f^{(n)}(i).$$

Intuitively, t represents the center starting point. $\underline{F}^{(n)}(t)$ counts number of events 30 seconds prior t and $\underline{F}^{(n)}(t)$ 30 post center point. Which covers the period of $[t-30, t+30]$.

$$G^{(n)}(t) = \begin{cases} 1 & \text{if} \quad \underline{F}^{(n)}(t) + \overline{F}^{(n)}(t) \geq 20 \\ 0 & \text{otherwise} \qquad . \end{cases}$$

$G^{(n)}(t)$ is indicator function satisfies requirement, that at least 20 licks must be present to consider as drinking bout.

$$\underline{T}^{(n)}(t_0) = \max\{t \leq t_0 : G^{(n)}(t) = 1 \ \wedge \ G^{(n)}(t-1) = 0\}$$

$$\overline{T}^{(n)}(t_0) = \min\{t \geq t_0 : G^{(n)}(t) = 1 \ \wedge \ G^{(n)}(t+1) = 0\} \tag{6}$$

where $\wedge$ is conjugation operation, $\overline{T}^{(n)}(t)$ gives timestamp of the start of the drinking bout and $\underline{T}^{(n)}(t)$ indicates the end of the drinking bout. Finally function can be constructed, which returns the duration of the drinking bout

$$\Gamma^{(n)}(t) = \begin{cases} \underline{T}^{(n)}(t) - \overline{T}^{(n)}(t) + t & \text{if} \quad (\underline{T}^{(n)}(t) - \overline{T}^{(n)}(t)) > 0 \\ 0 \quad \text{otherwise} \end{cases}$$

Function Γ aggregates drinking bouts as defined [26].

6.1.2 Neurophysiological data

During a single trial two channels were recorded for each rat. Three different rats were placed in separate cages, which had two lickometers in it with water and alcohol. Electrodes were attached to the brains and neurophysiological data were sampled at 1kHz interval. For one channel it makes 1000 data points per second. In total it makes 86400000 data points per 24h. For each rat two channels were recorded at a time making total number 172800000 of data points for a single rat. Since, during single trial normally three rats were analyzed that makes in total 518400000 data points recorded.

6.1.3 Technologies and implementation

LFPs were recorded using 6 channel biopotential amplifier *ISO DAM 8A* (World Precision Instruments WPI). Amplification coefficient x1000, using linear filter (bandwidth filter 0.1-100Hz) and 50Hz notch filter. Analog electrical signal was converted to digital using *Power 1401* (Cambridge Electronic Design, CED). Data were sampled using 16 bit ADC converter at 1kHz sampling rate. *Spike2* (Cambridge Electronic Design, CED) software was used, for signal recording.
Scripts for lickometer data clustering and LFP data import into database, were developed using *Python 2.7* programming language. *Microsoft SQL 2017 Database* running on *Windows Server 2016* operating system on virtual machine, was used for storing processed data.

Rstudio-server v1.0.153 on *Debian Jessie* linux distribution, running on virtual machine, was used. For FDA fda.usc [28] R package was used. WaveletComp [29] R package was used for CWT with modifications to apply for functional data.

6.2 Analysis

The proposed analysis of signals can be broken down into four distinct steps. First, neurophysiological signals of interest are smoothed by a continuous functions. Second, fitted functions are represented in the eigenbasis which are an orthonormal basis of the Hilbert Space L^2 that consists of the eigenfunctions of the autocovariance operator. Third, PCs were rotated using VARIMAX rotation technique. Finally, CWT is used to divide eigenfunctions into wavelets.
For this analysis an area of interest is four seconds long: **two seconds before the drinking bout and two seconds onwards** capture the first two seconds of drinking period. The critical point of interest is the first moment when the rat licked alcohol during the drinking bout. Let, be a sequence of timestamps of each drinking bout when lickometer was first triggered,

$$S^{(k)} = (\overline{T}^{(n)}(t) : \overline{T}^{(n)}(t) > 0)_{t=0}^{N}$$

where k is lickometer number, $N = 86400000$ and $\overline{T}^{(n)}$ is a function defined in (6). which returns the start time of the drinking bout.
Let,

$$Signal^{(m,k)} = \begin{bmatrix} X^m_{(S_1^{(k)}-2000)} & X^m_{(S_1^{(k)}-1999)} & \dots & X^m_{(S_1^{(k)}+2000)} \\ X^m_{(S_2^{(k)}-2000)} & X^m_{(S_2^{(k)}-1999)} & \dots & X^m_{(S_2^{(k)}+2000)} \\ \vdots & \vdots & \ddots & \vdots \\ X^m_{(S_n^{(k)}-2000)} & X^m_{(S_n^{(k)}-1999)} & \dots & X^m_{(S_n^{(k)}+2000)} \end{bmatrix}$$

where X^m denotes a vector with values recorded from brain activity and m is a rat number.

Figure 4 shows 6 intervals of signal data. Vertical red line indicates when drinking bout happened.

6.2.1 Data representation: smoothing

Smoothed functions are built up from basis functions $\phi_1(t), \dots, \phi_K(t)$. The important element to consider which basis system to use. Most popular are Fourier basis and b-splines. Fourier basis is defined by the basis functions $\phi_0 = 1$, $\phi_{2r-1} = \sin(rwt)$, $\phi_{2r} = \cos(rwt)$ Sine waves oscillate infinitely, thus these are well suited for periodic data, by nature neurophysiological data tend to be periodic. However, such data is highly unstable and reflect discontinuities. So Fourier series may be inappropriate because it generally yield expansions which are uniformly smooth. Therefore b-spline basis system was used, since b-slines can better capture abrupt changes and represent non-stationary signals.
The other parameter to consider is how many basis (K) are sufficient enough to properly represent discrete values. Although many methods are available to estimate the number of basis functions K, however due to nature of the data and information needed to retain, the value of K was chosen by trial and error, and equals to 99.
From raw data $Signal^{(m,k)}$ representing signal amplitude sampled at discrete time steps a smoothing approximation $x(t)$ is obtained as described in chapter 4.1 The figure 5 shows raw signal points and smoothed function $x(t)$

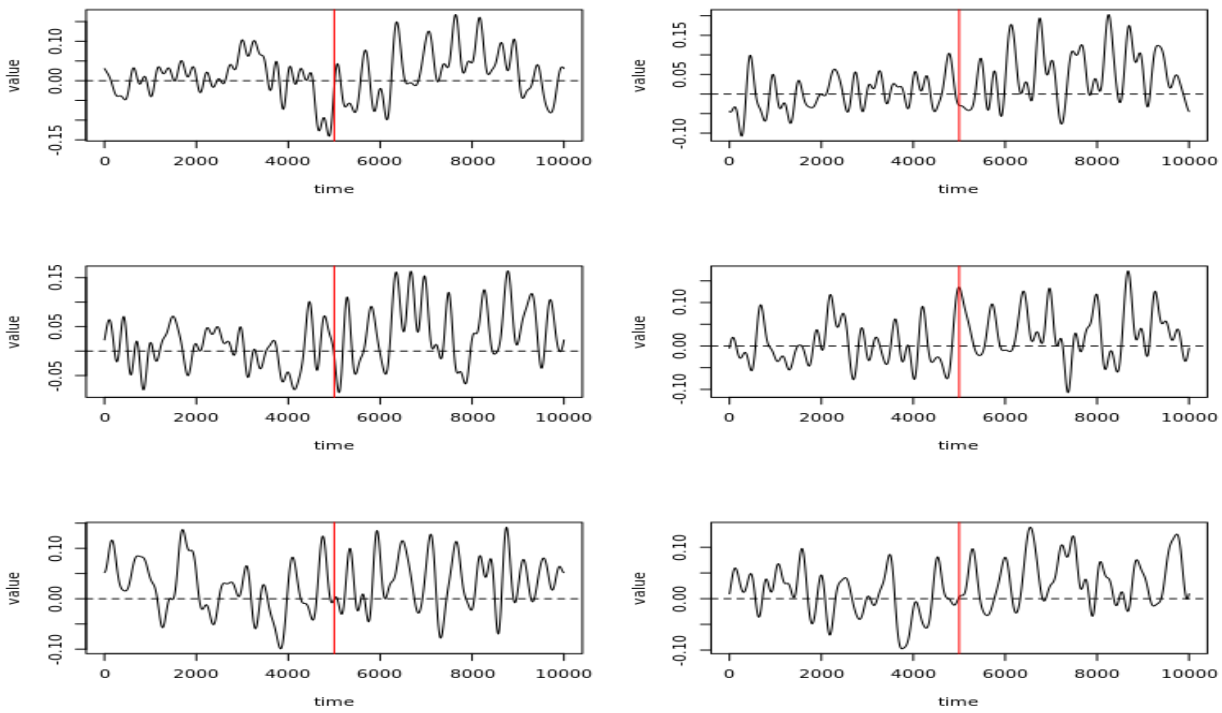

Figure 4: 10 seconds of raw neurophysiological data: 5s before drinking bout and 5s onwards. Red line indicates the moment when lickometer was triggered.

6.3 Dominant modes of variation

PCA is often the first method that follows after descriptive statistics. It helps to observe primary modes of variations which exists in the data. In multivariate case *eigenvalues* of the bivariate *variance-covariance function* are the indicators of the importance of these PC. Similarly, when working with functional data there exists an *eigenfunction* associated with each *eigenvalue*, instead of an *eigenvector*. These eigenfunctions describe major variational components. The formulation of fPCA is defined in chapter 4.2.
Having applied of fPCA technique showed that in trials where lamotrigine was not used, around 75% variability can be explained with 4 PCs (Figure 6a). Slightly higher variability exists in trial when rat received injection of Lamotrigine. It is worth stressing out that the explained variability by third PC among trials has smallest difference. In all cases thid PC explains almost the same amount of variability (around 5%). This component will play a crucial role in further analysis.

6.3.1 Visualizing the components

Interpreting the components may not be as straight-forward as in a multivariate case. Some technique, have to be considered that may aid their interpretation. Since PC represents *variation* around the mean, it is convenient to display the mean curve along +'s and -'s indicating the effect of adding and subtracting suitable multiple of the PC. When visualizing components, it is necessary to choose which multiple of the PC function to use. Define a constant C to be the root-mean-square difference between $\hat{\mu}$ and its overall time average,

$$C^2 = T^{-1}\|\hat{\mu} - \overline{\mu}\|$$

where

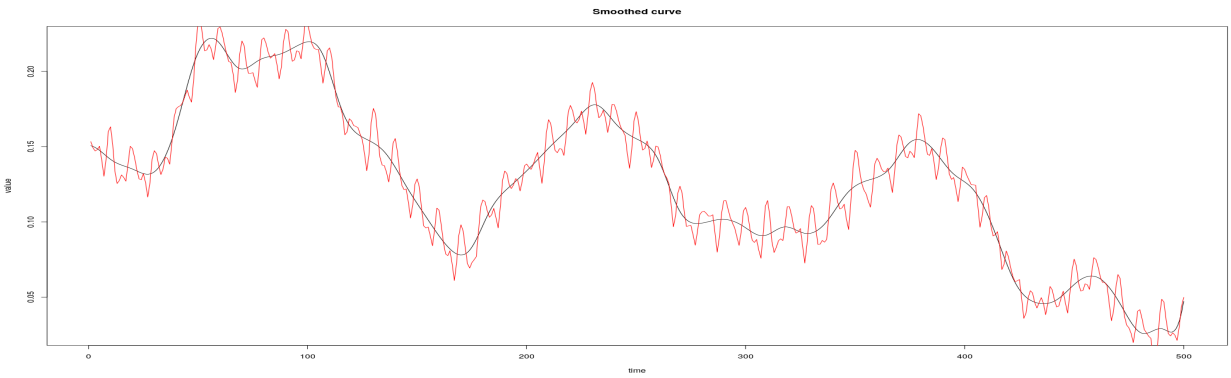

Figure 5: Smoothed signal. Black curve is a smoothed version of the signal plotted in red.

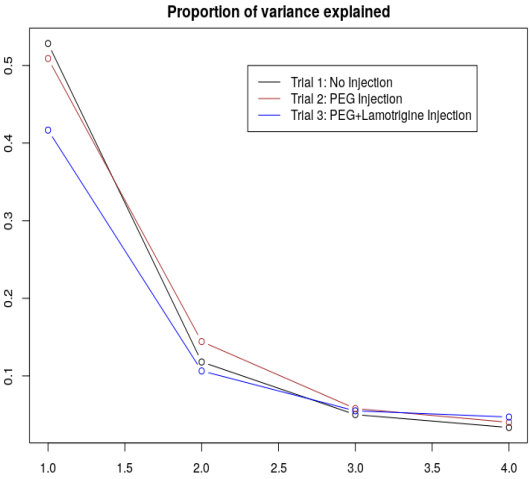

(a) Variance explained by each principal component for all trials.

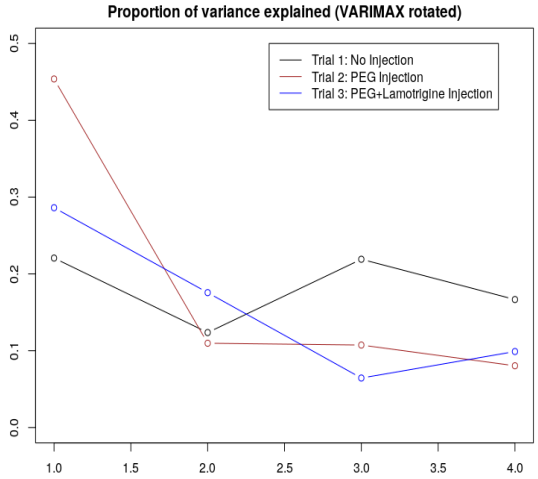

(b) Variance explained by each principal component for all trials (VARIMAX rotated).

$$\overline{\mu} = T^{-1} \int \hat{\mu}(t)\, dt.$$

When C is chosen as a constant equal to 0.2 it shows the effect of ± 2 standard deviations of each PC and gives interpretable results.

Figures A.12, A.13 (see appendix A) and 7 shows four principal components of trial 1, 2 and 3 respectively. In all trials the first component portrays variation that is strongest before the contact with alcohol whilst the second captures "more" variance during the contact with alcohol.

Moreover, plotting PC functions from each trial on the same chart may help to understand the differences between them. Figure A.12 (see appendix A) shows each PC function from all trials together. It is easy to see that the third PC has the highest differences among the trials, especially after the contact with alcohol. The blue line, which represents trial 3, has much stronger dynamics compared to the other trials. It is even more visibly distinguishable after taking a derivative of the third PC function as shown in figure 8. This may suggest that indeed lamotrigine effect can be detected from neural data.

6.3.2 Rotating principal components

In fPCA the weight functions ξ_m (2) can be viewed as defining an orthonormal set of K functions for expanding the curves to minimize a summed integrated squared error criterion

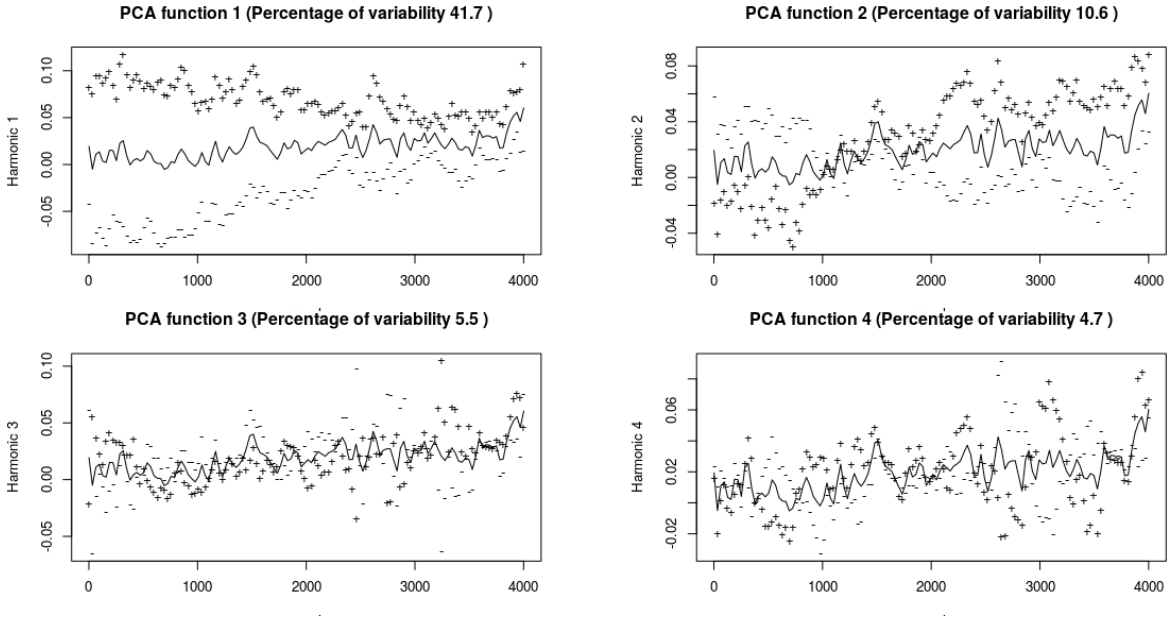

Figure 7: 4 PCs extracted from the trial when a rat was injected lamotrigine. Harmonics are shown as perturbations of the mean, which denoted by the solid line. The+'s show what happens when principal component is added to the mean, whilst -'s show the effect of subtracting the component.

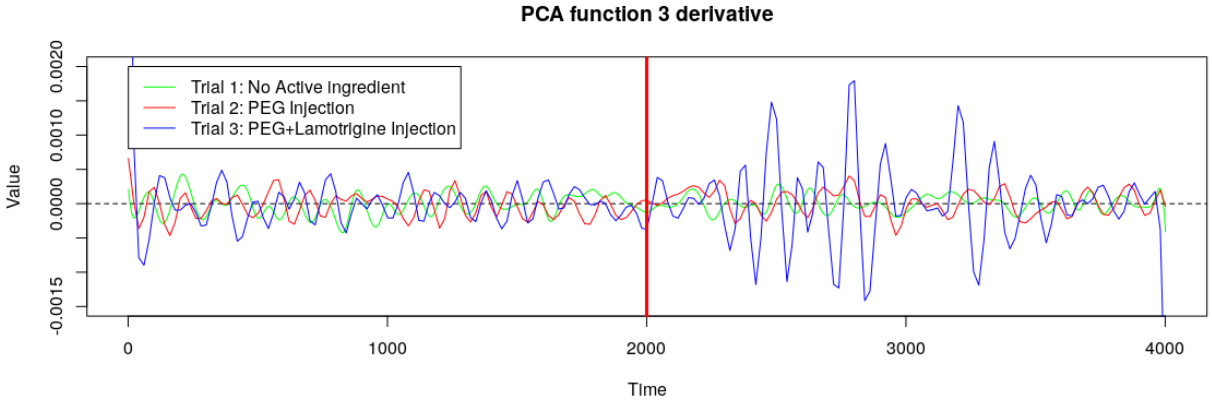

Figure 8: Derivative of the third PC function. Blue line, which represents the trial when rat was injected with lamotrigine, shows higher variation after the contact with alcohol.

[21]. This usually displays a similar sequence of variation independently of the data being analyzed. The first PC is normally a constant shift, the second PC is a linear contrast between the first and the second half with a single crossing of zero, the third quadratic pattern [30] and so on. That is tendency towards the sequence of orthogonal polynomials. This does not mean that there are no other orthonormal sets, which would be suitable as well. ξ can be defined as the vector-valued function $(\xi_1, \ldots, \xi_K)^\top$, then an equally good orthonormal set is defined by [21]

$$\psi = T\xi \tag{7}$$

where T is any orthonormal matrix of order K.

VARIMAX is a widely used orthonormal transformation in a multivariate analysis and can make multivariate PCs more interpretable. The rotations yield components that have either very high or very low values, effectively focusing variation on particular regions of the functional domain. The same concept can be applied in FDA.

Let $\mathbf{B}$ be a $K \times n$ matrix representing the first K PC functions $\xi_1, \ldots, \xi_K$. The corresponding matrix A of values of the rotated basis functions ψ (7) is given by

$$A = TB$$

where $B_{mj} = \xi_m(t_j), 1 \leq j \leq n$. Given an orthonormal matrix T, ψ (7) gives a new set of orthonormal functions. Denote the mjth entry of matrix A by a_{mj}. Then the VARIMAX strategy for choosing the orthonormal rotation matrix T is to maximize the variation in the values a_{mj}^2 over all values of m and j. The solution to the above maximization problem will encourage values a_{mj} to be either strongly positive, near zero, or strongly negative [31]. In algebraic terms,

$$\sum_m \sum_j a_{mj}^2 = \text{trace}\, A^\top A = \text{trace}\, B^\top T^\top T B = \text{trace}\, B^\top B.$$

It is not guaranteed that after rotation ψ_1 will define the largest component of variation, but a cumulative sum of the proportion of variance explained by each eigenfunction is equal to unrotated version. The resulting rotated functions ψ_m, along with the percentages of variances that they account for, are now quite different (figure 6b).
Figures 9, B.15 (appendix B), and B.16 (appendix B) shows four rotated PCs for trials 1,2 and 3 respectively. Although it does not show common pattern among the different trials, but analyzing each trial individually can reveal interesting segments and components which are responsible for the variation.

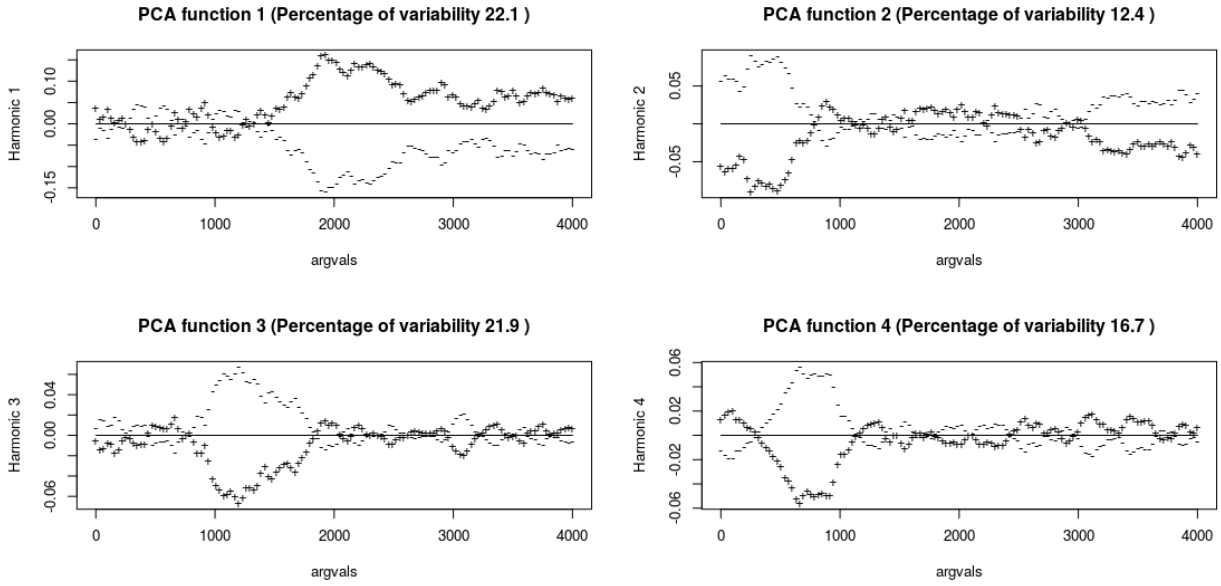

Figure 9: The data was centered on the mean function. VARIMAX rotated. Functional principal components extracted from trial when a rat was not injected with active substance. Each PC appears to be responsible for different time segments. Especially, seen in 1,2,3 PCs. The second PC is responsible for a process between 0ms and 1000ms, third PC responsible for the process between 1000ms and 2000ms. The first PC is responsible for the process between 2000ms and 4000ms.

Figure 9 shows 4 PC functions from the first trial

1. The first PC accounts for variability between 2000ms to 4000ms, which is the moment when rat was drinking alcohol.

2. The second PC accounts for variability between 0ms to 1000ms and 3000ms to 4000ms.

3. The third PC accounts for variability between 1000ms to 2000ms. This may be the most interesting component to understand since it may capture the variation of the moment when a rat made a decision to drink alcohol.

Figure B.15 shows 4 PC functions which is from the second trial when a rat was injected with PEG. Again, different time segments are explained by different PCs.

1. The first PC accounts for variability between 500ms to 1500ms.
2. Then second PC accounts for variability between 0ms to 1000ms and 3000ms to 4000ms and is a very similar to the first trial.
3. The third PC accounts for variability between 1500ms to 2500ms, and is also, similar to the first trial.

Figure B.16 (appendix B) shows 4 PC functions which is from the third trial when a rat was injected with PEG and Lamotrigine. It has slightly, different pattern. Only first two components represent distinguishable segments. The first PC accounts for variability between 0ms to 1000ms and the second PC accounts for variability between 1000ms to 4000ms. The third and the fourth components do not strongly distinct any interpretative pattern.
Such clear segmentation can be very powerful for understanding brain dynamics leading to decision making process.
The exploratory analysis described above reveals clear structural changes and patterns that can be distinguished based on whatever rat was injected with an active substance or not. However, it does not capture the dynamics in frequency domain. Also, more analytical approach is needed to highlight the significance of changes in rhythmic activities. Calculating correlations only between principal component functions of each trial would not give a robust evidence, because only one function per trial can be extracted within the given dataset. This motivates to apply wavelet analysis.

6.4 Wavelet analysis

Wavelet analysis is performed by projecting the signal to be analyzed on the wavelet function. It implies a multiplication and an integration as defined in equation (4). The strength of the wavelet analysis is that it allows changing the size of the function, to make it suitable for the targeted resolution in time or frequency domain.
Each PC function was processed with the CWT using Morlet wavelet as the mother wavelet defined in equation (5) for every trial.
The local amplitude of any periodic component of the time series and changes over the time domain can be calculated by modulus operation of its wavelet transform. The square of the amplitude has an interpretation as time-frequency (or time-period) wavelet energy density, and is called the wavelet power spectrum. It can be defined as

$$P(\tau, s) = s^{-1} \cdot |\Phi_{k,x}(\tau, s)|$$

where $\Phi_{k,x}$ is a corresponding wavelet transform (4) of the k-th PC ξ_k of the x-th trial, s is a scale factor and τ is a mother wavelet translation in time.

6.4.1 Wavelet power spectrum interpretation

Before moving to wavelet power spectrum plots it is worth stressing out that an attention should be paid to two separate segments divided by middle vertical red line, which separates 2 seconds before s contact with alcohol and 2 seconds onward when rat was consuming alcohol. The differences between those two segments reveal behavior changes influenced by alcohol in brain wave.
The power spectrum plot in Figure C.18 (appendix C) was made from the first PC (ξ_1) of each trial. The color bar reveals the steep power gradient. It might be tempting to assume that trial 1 and trial 2 power spectrum plots share a similar pattern; however, the attention should be paid in the power spectrum scale. Trial 1 and Trial 3 power range is from 0.0 to 0.1 while trial 2 has a stronger power levels from 0.0 to 0.3. The power ridge patterns also constitute the black lines has similar pattern around 512 period and ridge line around period 2000 is present in all trials.
Figure (C.19) was made from the second PC (ξ_2). Here, the power spectrum scale becomes stronger in trial 1 and trial 2. More similarities show up between trial 1 and trial 2.

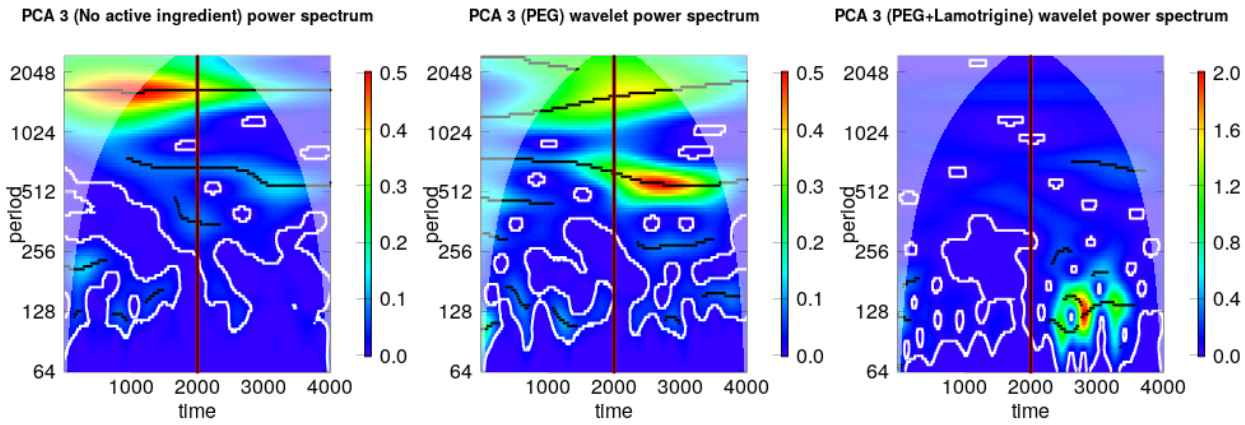

Figure 10: CWT on the third PC displays differences among trials. While trial 1 and 2 have similar patterns and power spectrum scale, the third PC shows 4 times stronger power scale especially in the lower right side.

The figure 10 (appendix C) was made from the third PC (ξ_3). As discussed and seen in the previous plots, this component may be responsible for a variability of the effect of the medicine. Interestingly now the power spectrum scale is the same for trial 1 and trial 2; however, it is four times stronger in trial 3. The similarities between first two trials can be visually evaluated. The black ridge lines between periods 512-1024 and 1024-2048 shows very similar patterns where lamotrigine was not injected.
Finally, figure C.20 was made from the fourth PC (ξ_4). Here, the power spectrum scale differs within each trial. Although, there is no evidence to support it from physiological perspective, but PEG might have some influence, since the similarities can be seen between trial 2 and trial 3. It is difficult to say whether it is caused by PEG injection.

6.4.2 Coherence analysis

While wavelet power spectrum plots reveal similarities and differences it is not sufficient evidence to support the hypothesis about lamotrigine effect. It lacks apparent quantitative results. The wavelet transform was regarded by many as an interesting diversion that produces colorful pictures, yet purely qualitative results [32]. More quantitative results can be achieved by calculating a coherence of frequency contents of PCs.

The concepts of cross-wavelet analysis provide appropriate tools for comparing the frequency contents of two signals. In this case, comparing PCs from different trials can reveal synchronicity at a certain periods and across certain ranges of time. The cross-wavelet transform of two k-th ($k = 1 \dots 4$) PCs $\xi_{k,x}(t)$ and $\xi_{k,y}(t)$ of the x-th trial and the y-th trial for $x \neq y$, with respective wavelet transforms $\Phi_{k,x}(\tau, s)$ and $\Phi_{k,y}(\tau, s)$ (4), decomposes the Fourier quadrature-spectra in time-frequency domain [33] can be defined as
Let,

$$W_{k,xy}(\tau, s) = s^{-1} \cdot \Phi_{k,x}(\tau, s) \cdot \Phi_{k,y}(\tau, s)$$

Cross-wavelet power can be calculated by its modulus:

$$P_{k,xy}(\tau, s) = |W_{k,xy}(\tau, s)|$$

The covariance depends on the unit of measurement, thus making it harder to interpret with regard to the degree of association, but wavelet coherency may remedy this. The concept of Fourier coherency measures the cross-correlation between two time series as a function of frequency; an analogous concept in wavelet theory [34]:

$$Coh_{k,xy}(t) = \frac{W_{k,xy}(t)}{\sqrt{P_{k,x}(t) \cdot P_{k,y}(t)}}, 0 \leq |Coh_{xy}(t)|^2 \leq 1.$$

In a geometric sense, the cross-wavelet transform is the analog of the covariance.

6.4.3 Coherence interpretation

For each trial's PC ξ_k for ($k = 1 \dots 4$) coherence was computed and respective figures (D.21, D.22, 11, D.23) display the results. Each figure has three plots that display the coherence between trials:

1. $Coh_{1;1,2}$ Compare trial 1 with trial 2
2. $Coh_{k;1,3}$ Compare trial 1 with trial 3
3. $Coh_{k;2,3}$ Compare trial 2 with trial 3

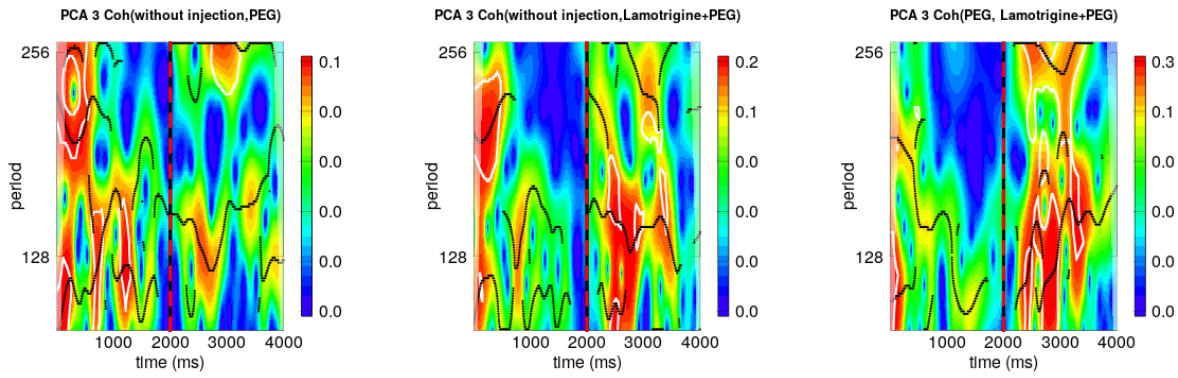

Figure 11: Coherence analysis of the third PC. The weakest correlations were found between trials (the first plot) with no medicine injected. Without medication stronger correlations are seen in the first segment (0s-2s). In trials where drug was injected the stronger correlation is seen in the second segment.

The reader should pay attention to the scale of power levels. While correlations plotted in the figures D.21, D.22 (appendix D) has almost no correlation, the third PC (figure 11) display stronger power levels, especially when comparing trial 1 with trial 3 and trial 2 with trial 3. Since in both cases the lamotrigine was involved it may suggest that the coherence is the result of the effect of the drug. It is easy to see that the first plot, which is a correlation between the first and second trials, shows stronger coherence at the first segment (0-2000ms), while the other two plots shows a weak coherence especially in upper periods(150-256). On the second segment (2000ms-4000ms) the effect is reverse: the first plot shows a weaker coherence whilst other two plots display stronger coherence, especially in the lower periods (100-150). The region of wavelet coherence significance periods at level 0.05 are within the white lines.

6.5 Discussion

From a statistical point of view, it is clear that different brain wave behavior can be detected in different trials. However, it seems that stronger correlations exist between trial 2 and trial 3, where PEG was injected. Although the US Food and Drug Administration have identified PEG as being "generally recognized as safe" at regulated concentrations [35] suggesting that it should have no impact, but there are studies claiming that in rat brains cell death triggered by PEG was found to have morphological characteristics of apoptosis [36] especially the damage was concentrated in the CPu brain region, is a result it may have affected brain waves. Whatever, the differences of brain behavior are caused by drug or PEG it's beyond the scope of this study.

7 Conclusions

This study introduces the approach on how brain processes can be separated and individually analyzed. Applying Functional Principal Component Analysis theory background brain work and noise can be separated and variability, which is caused by drug can be analyzed independently. In combination with VARIMAX rotation distinct process timeline was identified. Such transformation is very convenient, since it does not change the frequencies allowing to explain the effect on the brain wave frequencies in the sense that is commonly used in neuroscience community. In addition, retaining the information about frequency power distribution and location can help to synthetically generate data for simulations giving the main ingredient for development of more robust statistical methods and tests.
Visually and analytically lamotrigine effect was detected in neurophysiological signals. Such conclusion in an agreement with the knowledge of importance of glutamate system in the neural and behavioral actions of alcohol.
Finally, a measurement of the background brain process variability was introduced. The analysis of PCs showed that background brain process account of for roughly 60% of variability.

References

[1] A brief history of biosignal-driven art. `http://econtact.ca/14_2/ortiz_biofeedback.html`. [Online; accessed 11-December-2017].

[2] Edmund Kaiser, Ingemar Petersén, Ulla Selldén, and Nina Kagawa. Eeg data representation in broad-band frequency analysis. *Electroencephalography and Clinical Neurophysiology*, 17(1):76 – 80, 1964.

[3] V.A. Kozhevnikov. Some methods of automatic measurement of the electroencephalogram. *Electroencephalography and Clinical Neurophysiology*, 10(2):269 – 278, 1958.

[4] Ognen A. C. Petroff. Book review: Gaba and glutamate in the human brain. *The Neuroscientist*, 8(6):562–573, 2002. PMID: 12467378.

[5] René H. Levy, Richard H. Mattson, and Brian S. Meldrum. *Antiepileptic Drugs*. Wolters Kluwer, 2015.

[6] Dailymed - lamotrigine chewable dispersible tablet, for suspension. `https://dailymed.nlm.nih.gov/dailymed/drugInfo.cfm?setid=05cba628-b12c-44d8-89a8-3522fe417cc1`. [Online; accessed 11-December-2017].

[7] Yi-Chyan Chen and Andrew Holmes. Effects of Topiramate and Other Anti-Glutamatergic Drugs on the Acute Intoxicating Actions of Ethanol in Mice: Modulation by Genetic Strain and Stress. *Neuropsychopharmacology*, aop(current), 2009.

[8] PhD Guochuan Tsai, MD and MD Joseph T. Coyle. The role of glutamatergic neurotransmission in the pathophysiology of alcoholism. *Annual Review of Medicine*, 49(1):173–184, 1998. PMID: 9509257.

[9] Louis Trevisan, Lawrence W. Fitzgerald, Nils Brose, Gregory P. Gasic, Stephen F. Heinemann, Ronald S. Duman, and Eric J. Nestler. Rapid communication chronic ingestion of ethanol up-regulates nmdar1 receptor subunit immunoreactivity in rat hippocampus. *Journal of Neurochemistry*, 62(4):1635–1638, 1994.

[10] Göran Engberg and Mihály Hajós. Ethanol attenuates the response of locus coeruleus neurons to excitatory amino acid agonists in vivo. *Naunyn-Schmiedeberg's Archives of Pharmacology*, 345(2):222–226, Feb 1992.

[11] Lawrence D. Snell, Boris Tabakoff, and Paula L. Hoffman. Radioligand binding to the n-methyl-d-aspartate receptor/ionophore complex: alterations by ethanol in vitro and by chronic in vivo ethanol ingestion. *Brain Research*, 602(1):91 – 98, 1993.

[12] Workshop on Stochastic Methods in EEG Research (1967.), (ed.) Walter, Donald O., 1904-(ed.) Brazier, Mary A. B. (Mary Agnes Burniston), and Los Angeles. Brain Information Service University of California. Advances in eeg analysis, 1969. Sponsored by the UCLA Brain Information Service.

[13] P. Jahankhani, V. Kodogiannis, and K. Revett. Eeg signal classification using wavelet feature extraction and neural networks. In *IEEE John Vincent Atanasoff 2006 International Symposium on Modern Computing (JVA'06)*, pages 120–124, Oct 2006.

[14] F. Carbonell, L. Galán, P. Valdés, K. Worsley, R.J. Biscay, L. Díaz-Comas, M.A. Bobes, and M. Parra. Random field–union intersection tests for eeg/meg imaging. *NeuroImage*, 22(1):268 – 276, 2004.

[15] Simona Carrubba, Clifton Frilot, Andrew Chesson, and Andrew A. Marino. Detection of nonlinear event-related potentials. *Journal of Neuroscience Methods*, 157(1):39 – 47, 2006.

[16] Hojjat Adeli, Ziqin Zhou, and Nahid Dadmehr. Analysis of eeg records in an epileptic patient using wavelet transform. *Journal of Neuroscience Methods*, 123(1):69 – 87, 2003.

[17] Z. Nenadic and J. W. Burdick. Spike detection using the continuous wavelet transform. *IEEE Transactions on Biomedical Engineering*, 52(1):74–87, Jan 2005.

[18] Hafeez Ullah Amin, Aamir Saeed Malik, Rana Fayyaz Ahmad, Nasreen Badruddin, Nidal Kamel, Muhammad Hussain, and Weng-Tink Chooi. Feature extraction and classification for eeg signals using wavelet transform and machine learning techniques. *Australasian Physical & Engineering Sciences in Medicine*, 38(1):139–149, Mar 2015.

[19] R. Panda, P. S. Khobragade, P. D. Jambhule, S. N. Jengthe, P. R. Pal, and T. K. Gandhi. Classification of eeg signal using wavelet transform and support vector machine for epileptic seizure diction. In *2010 International Conference on Systems in Medicine and Biology*, pages 405–408, Dec 2010.

[20] Carl De Boor. *A practical guide to splines*. Springer, 2001.

[21] James O. Ramsay and B. W. Silverman. *Functional data analysis*. Springer, 2006.

[22] Ioana Adam. *Complex Wavelet Transform: application to denoising*. PhD thesis, Politehnica University of Timisoara and Université de Rennes, 2010.

[23] Buzsaki Gyorgy. *Rhythms of the brain*. Oxford University Press, 2011.

[24] Xiaobin Zhuang, Yuanqing Li, and Nengneng Peng. Enhanced automatic sleep spindle detection: a sliding window-based wavelet analysis and comparison using a proposal assessment method. *Applied Informatics*, 3(1):11, Dec 2016.

[25] Charles K. Chui. *An Introduction to Wavelets*. Academic Press Professional, Inc., San Diego, CA, USA, 1992.

[26] A. M. Barkley-Levenson and J. C. Crabbe. Distinct ethanol drinking microstructures in two replicate lines of mice selected for drinking to intoxication. *Genes, Brain and Behavior*, 15(3):356–356, 2016.

[27] Matthew M. Ford, Ethan H. Beckley, Jeffrey D. Nickel, Sarah Eddy, and Deborah A. Finn. Ethanol intake patterns in female mice: influence of allopregnanolone and the inhibition of its synthesis. *Drug and alcohol dependence*, 97(1-2):73–85, September 2008.

[28] Manuel Febrero-Bande and Manuel Oviedo de la Fuente. Statistical computing in functional data analysis: The R package fda.usc. *Journal of Statistical Software*, 51(4):1–28, 2012.

[29] Angi Roesch and Harald Schmidbauer. *WaveletComp: Computational Wavelet Analysis*, 2014. R package version 1.0.

[30] James Ramsay, Giles Hooker, and Spencer Graves. *Functional Data Analysis with R and MATLAB*. Use R. Springer, 1 edition, July 2009.

[31] Chong Liu, Surajit Ray, Giles Hooker, and Mark Friedl. Functional factor analysis for periodic remote sensing data. *Ann. Appl. Stat.*, 6(2):601–624, 06 2012.

[32] Christopher Torrence and Gilbert P. Compo. A practical guide to wavelet analysis. *Bulletin of the American Meteorological Society*, 79(1):61–78, 1998.

[33] Doris Veleda, Raul Montagne, and Moacyr Araujo. Cross-wavelet bias corrected by normalizing scales. *Journal of Atmospheric and Oceanic Technology*, 29:1401–1408, 09 2012.

[34] Paul C. Liu. Wavelet spectrum analysis and ocean wind waves. *Wavelets in Geophysics Wavelet Analysis and Its Applications*, page 151–166, 1994.

[35] Food and drug administration. gras status of propylene glycol and propylene glycol monostearate. *Fed Regist.* 1982;47:27810.

[36] Karen Lau, Brant S. Swiney, Nick Reeves, Kevin K. Noguchi, and Nuri B. Farber. Propylene glycol produces excessive apoptosis in the developing mouse brain, alone and in combination with phenobarbital. *Pediatric Research*, 71(1):54–62, 2012.

Appendices

A Figures for Functional Principal Component analysis

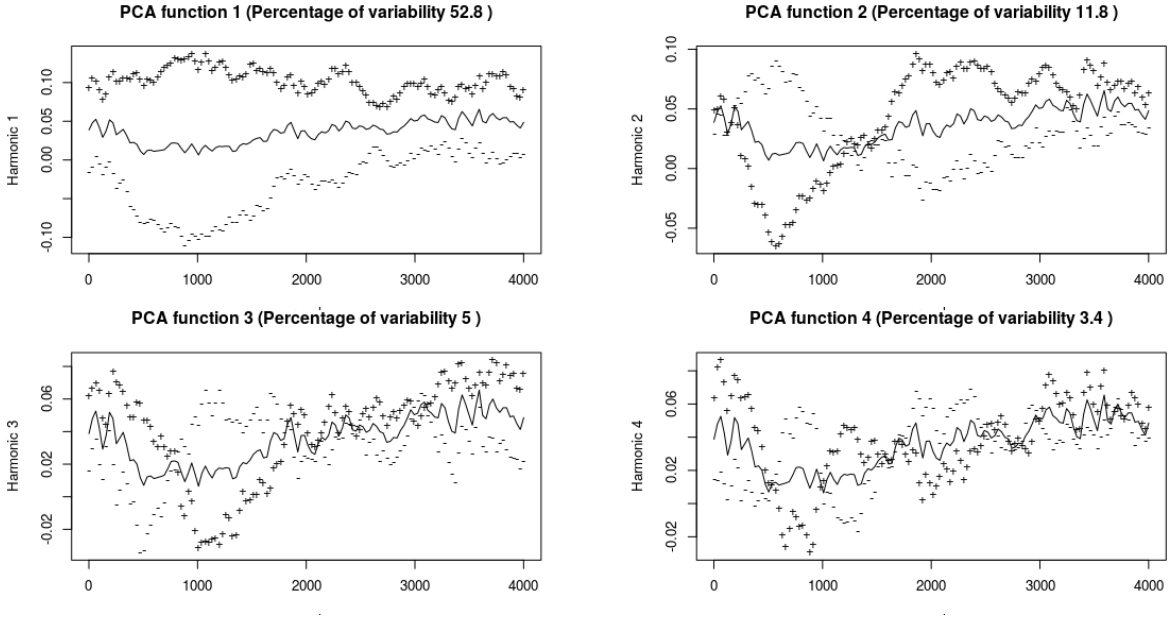

Figure A.12: Functional principal components extracted from trial when a rat was not injected any active substance. Harmonics are shown as perturbations of the mean, which denoted by solid line.

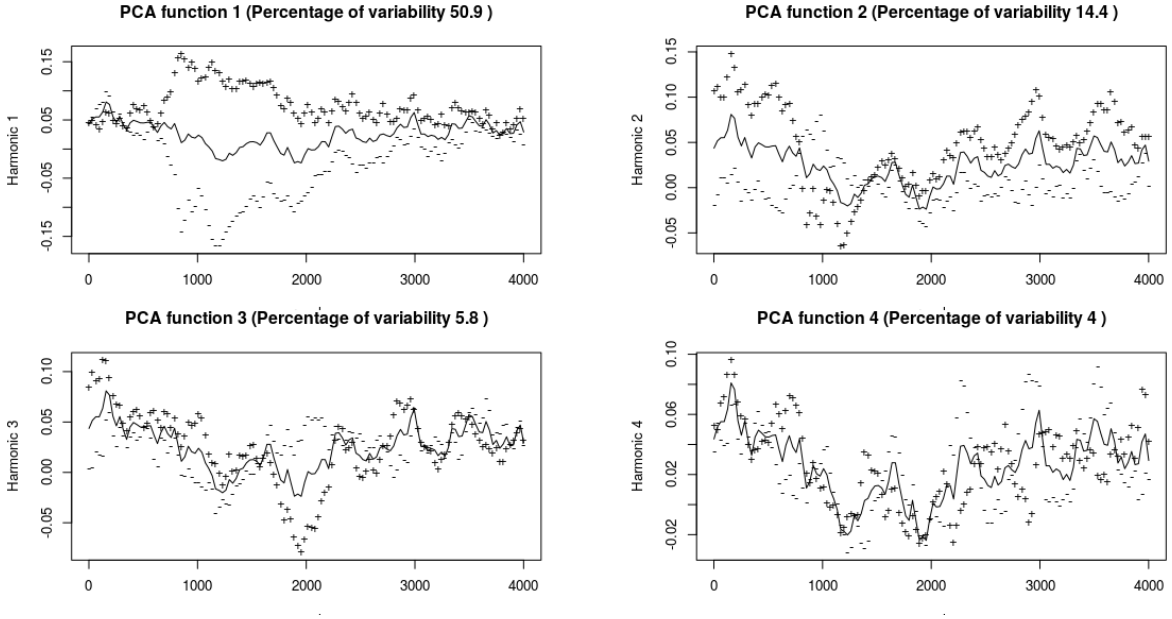

Figure A.13: Functional principal components extracted from trial 2 when a rat was injected with PEG.

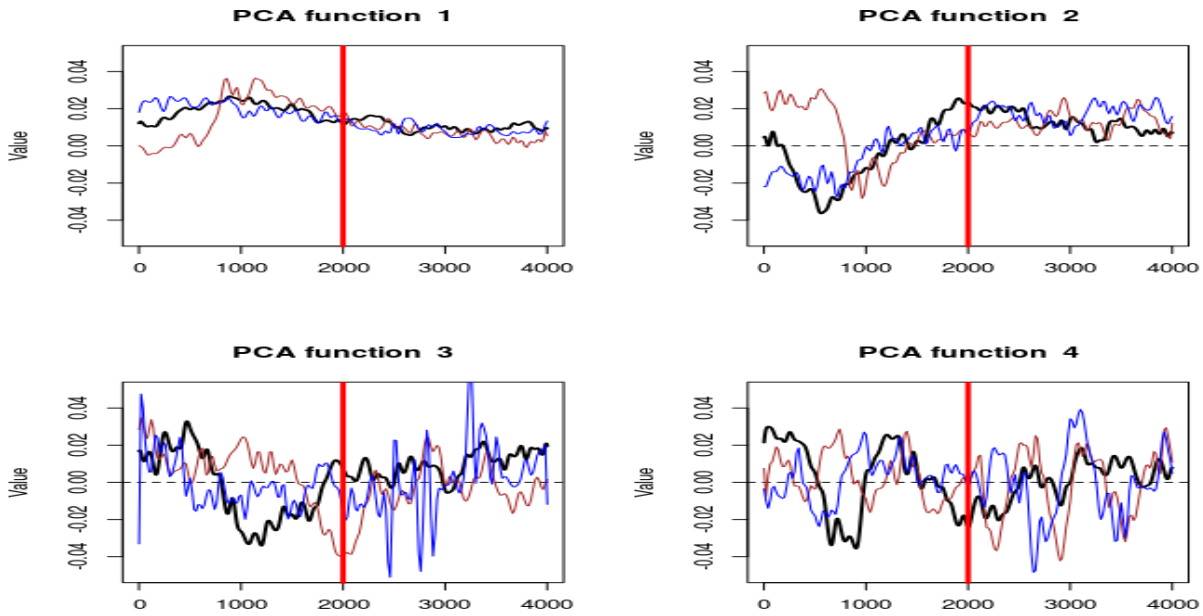

Figure A.14: PC functions from each trial. Black line (Trial 1), Brown line (Trial 2), Blue line (Trial 3). While PCs 1 and 2 display similar pattern, the third PC shows a stronger dynamics for trial 3, when a rat was injected with lamotrigine.

B Figures for VARIMAX rotated Functional Principal Component analysis

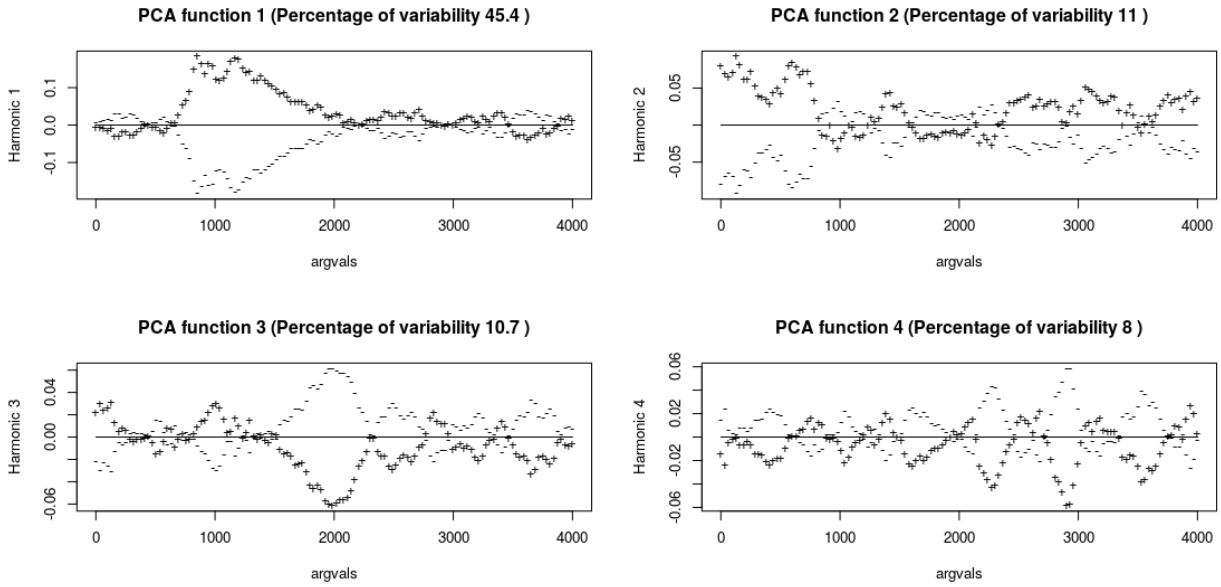

Figure B.15: The data was centered on the mean function. VARIMAX rotated. PCs extracted from trial 2 when rat was injected with PEG.

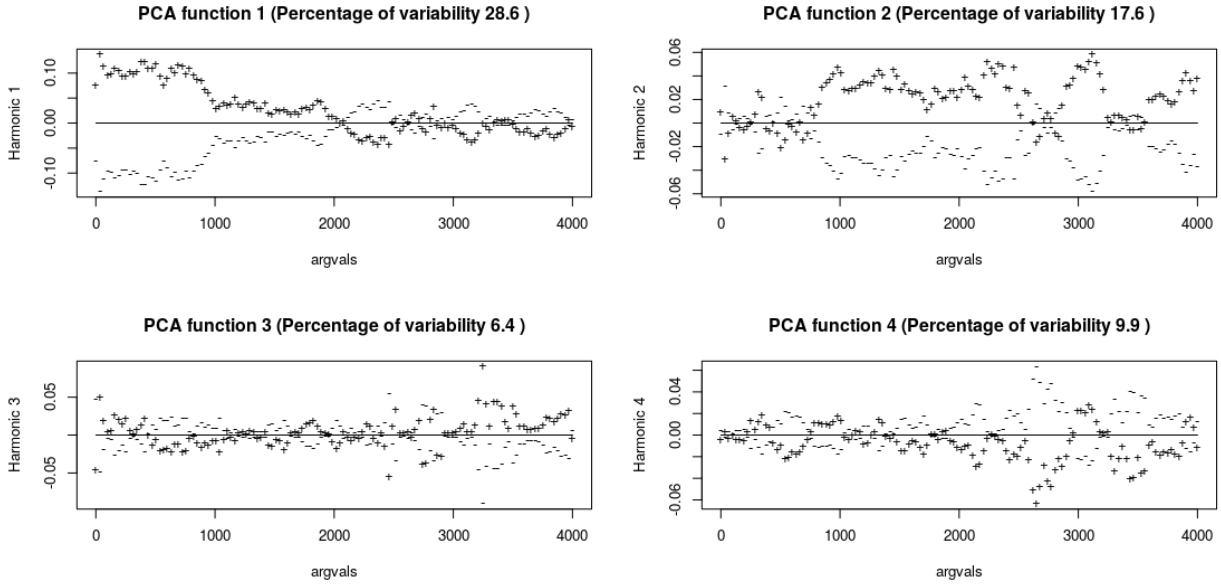

Figure B.16: The data was centered on the mean function. VARIMAX rotated. PCs extracted from trial 3 when rat was injected with active substance.

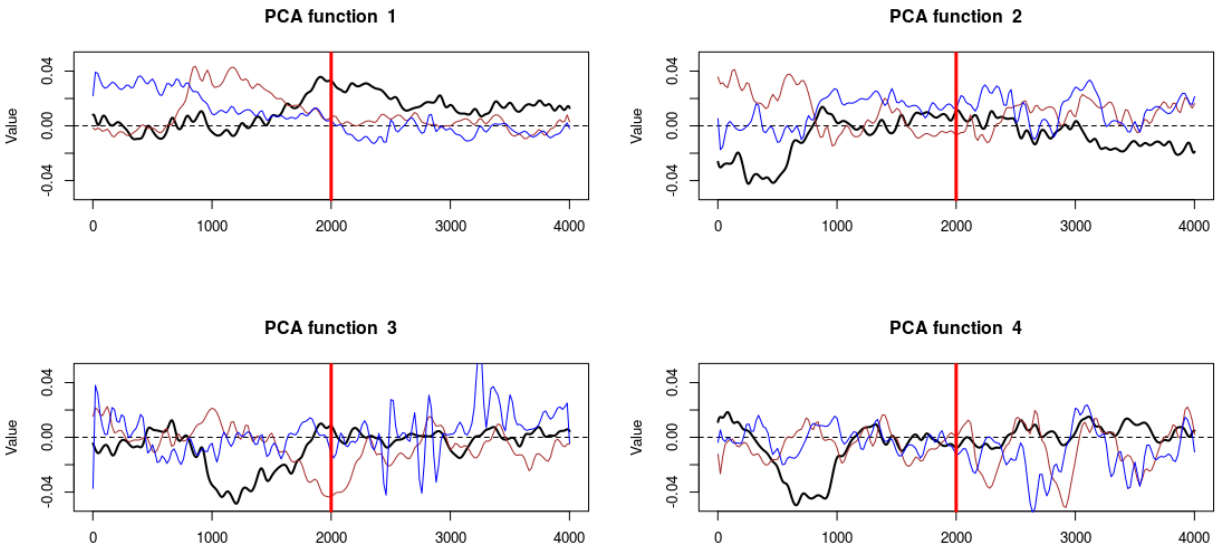

Figure B.17: PCs after VARIMAX rotation: Black line (Trial 1), Brown line (Trial 2), Blue line (Trial 3). PC 3 shows a stronger dynamics in trial 3.

C Figures for wavelet power spectrum analysis

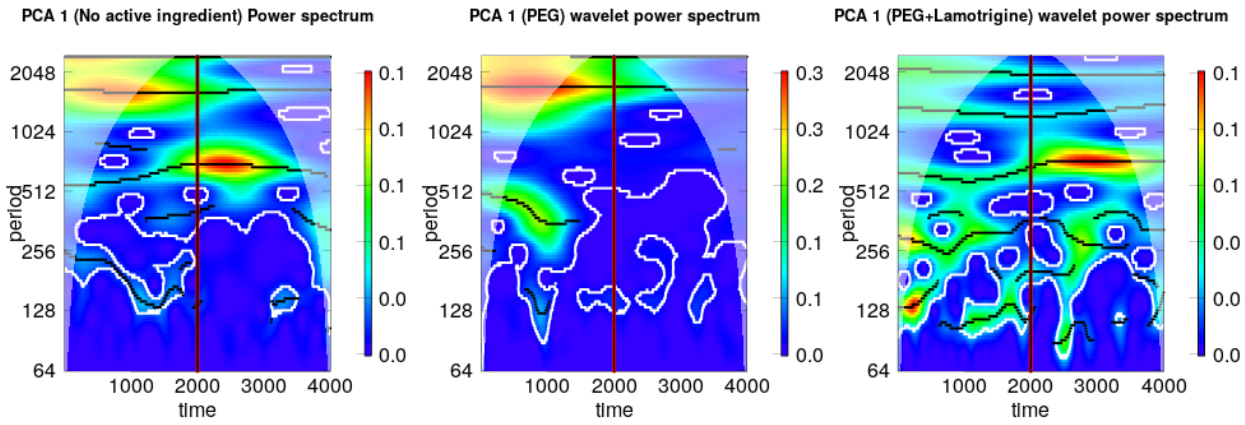

Figure C.18: CWT of the first PC (ξ_1) for each trial, display wavelet power spectrum.

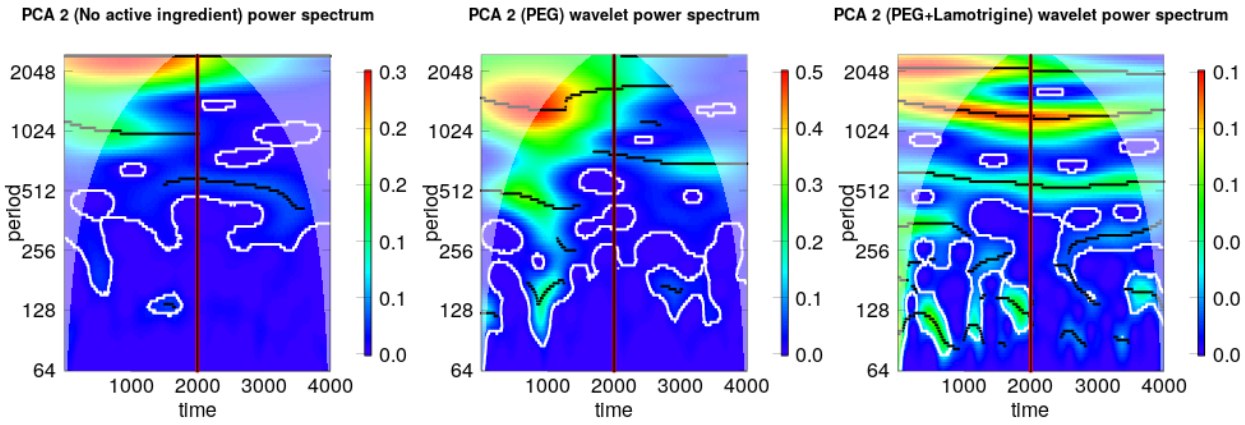

Figure C.19: CWT of second PC (ξ_2) for each trial, display wavelet power spectrum

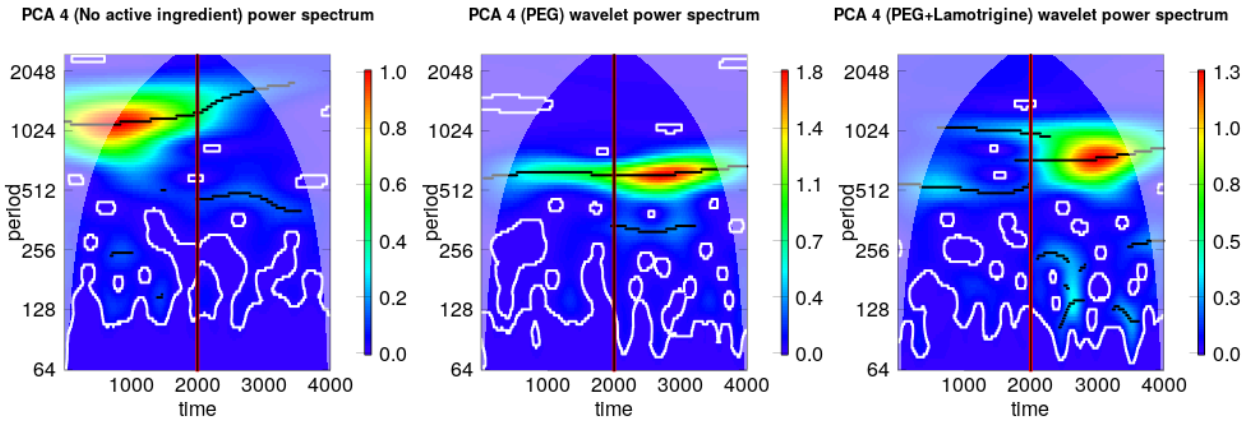

Figure C.20: CWT of fourth PC (ξ_4) for each trial, display wavelet power spectrum

D Figures for Functional Principal Component coherence analysis

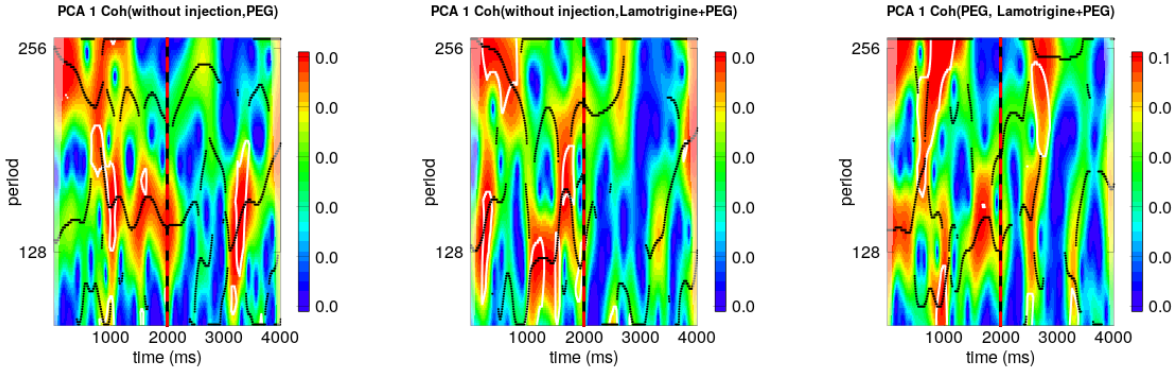

Figure D.21: Coherence analysis of the first PC (ξ_1) for each trial.

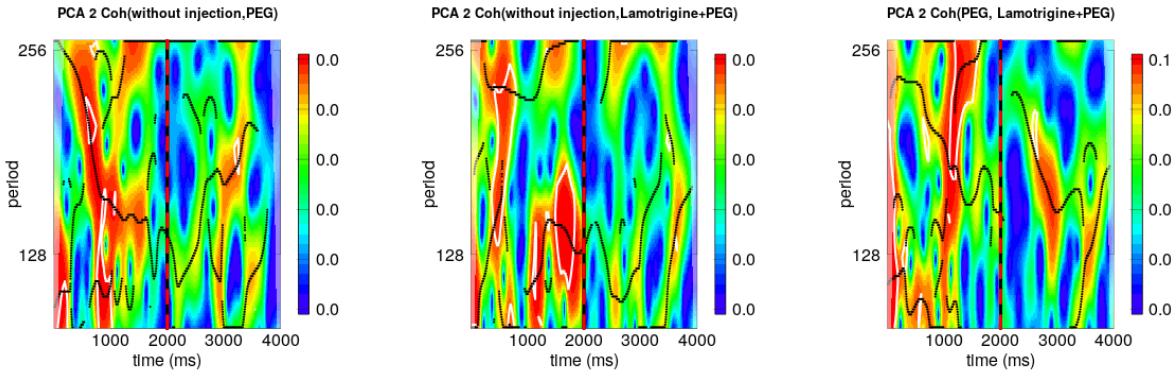

Figure D.22: Coherence analysis of second PC (ξ_2) for each trial.

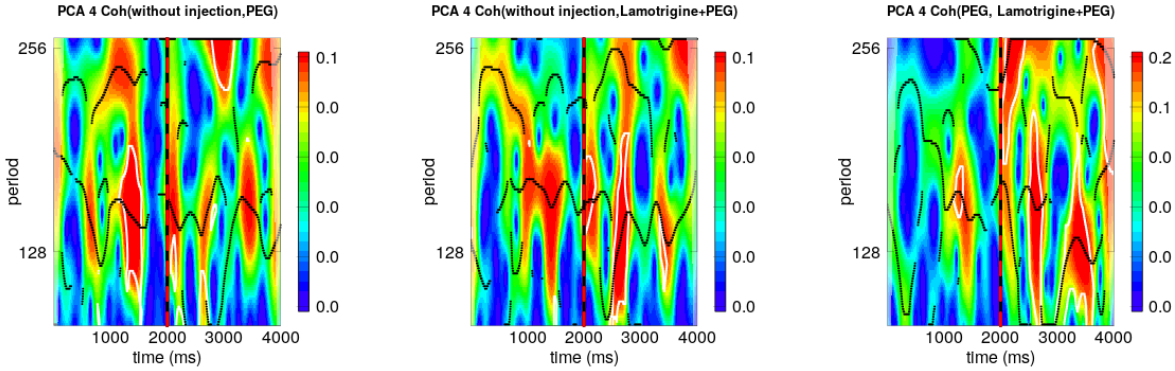

Figure D.23: Coherence analysis of fourth PC (ξ_4) for each trial.